ELSEVIER

1 February 2002

Optics Communications 202 (2002) 199–204

OPTICS COMMUNICATIONS

www.elsevier.com/locate/optcom

Intensity-dependent temporal laser pulse shaping and propagation in ZnSe

Yingxin Bai, P.P. Ho, R.R. Alfano *

Department of Electrical Engineering and Physics, The Institute for Ultrafast Spectroscopy and Lasers, The City College of New York, 138th Street and Convent Avenue, New York, NY 10031, USA

Received 24 January 2001; received in revised form 26 September 2001; accepted 12 November 2001

Abstract

The shape of a 40-ps 1064-nm laser pulse propagating through ZnSe at different intensities was investigated using a single-shot optical Kerr gate. At high intensity ~3.65 GW/cm^2, the pulse peak moves forward in time by about 15 ps from the position at low intensity and the full width at half maximum reduces from 40 to 27 ps. This pulse advancement and time shortening are attributed to a combination of two-step absorption and negative nonlinear dispersion. The numerically simulated results based on these two processes are in good agreement with the experimental results. © 2002 Published by Elsevier Science B.V.

PACS: 42.70.M; 42.65.R; 42.25.B; 78.20.C

Keywords: Nonlinear; Dispersion; Pulse compression

II–VI semiconductors are important materials for many photonic applications. ZnSe has excellent physical, chemical and nonlinear optical properties as well as low absorption spanning from the red to the infrared. Consequently, it is thought of as one of the most promising optical materials for many practical optical functions such as Tera hertz generation, optical limiting, all-optical switching, displays and optical memory elements [1–6]. An anomalous spectral broadening has been observed in ZnSe, larger for Stokes than anti-Stokes [7].

In this paper, the intensity-dependent reshaping of a 40 ps laser pulse through a ZnSe plate was investigated using an improved single-shot optical Kerr gate. Based upon a two-step absorption with negative nonlinear dispersion model, the experimental results were simulated.

The schematic arrangement for a single-shot optical Kerr gate (SOKG) technique is shown in Fig. 1. A mode-locked Nd:YAG laser was used to generate 1064 nm and 532 nm pulse of 40 and 30 ps, respectively. The 30-ps 532-nm probe pulse was passed onto a ~90° blazed reflection grating to be transformed into an oblique temporal front converting a 200 ps temporal window. A lens was used to focus the probe beam into a 1 mm long CS_2 Kerr cell to form an extended probing time base.

* Corresponding author. Fax: +1-212-650-5530.
E-mail address: alfano@scisun.sci.ccny.cuny.edu (R.R. Alfano).

0030-4018/02/$ - see front matter © 2002 Published by Elsevier Science B.V.
PII: S0030-4018(01)01699-6

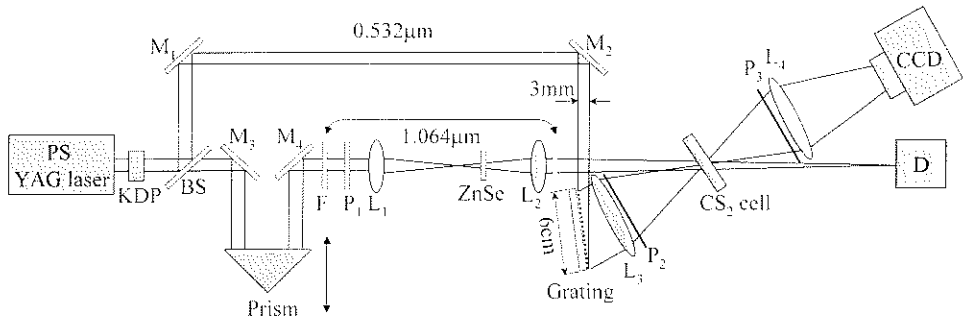

Fig. 1. Single-shot optical Kerr gate experimental setup. A mode locked YAG laser generates the 1064 nm laser pulses of ~40 ps in FWHM, the laser pulses pass through the second harmonic crystal (KDP) generating 532 nm laser pulses of ~30 ps in FWHM. These pulses are split into a pumping beam (1064 nm) and a probing beam (532 nm) by a beam splitter (BS). The probing beam reflected by mirrors M_1 and M_2 reaches a 6 cm long 90° blazed grating with 1800 lines/mm. For improving the spatial uniformity of the probing beam only a 3 mm central portion of the 9 mm diameter probing beam is diffracted into a ~200 ps oblique wave front. The segmented pulse passes through lens L_3, the Kerr gate and lens L_4 and reaches a cooled charge coupled device (CCD) camera with 1024 × 1024 pixels and a 16 bit dynamic range. This pulse is used to probe the 1064 nm pulse profile. The Kerr-gate is composed of a pair of crossed Polaroid (HN22) polarizers P_2 and P_3 and a 1 mm thick CS_2 cell located at the focal point of lens L_3 as the Kerr medium. The focal lengths of lens L_3 and L_4 are 20 cm. The pumping beam passes into a delay line composed of mirrors M_3 and M_4 and a movable prism and passes through a series of neutral density filters (F) and a 30-cm focal length lens (L_1) into the ZnSe sample. The 1064 nm pumping beam passes through another 30-cm focal length lens L_2 and meets the 532 nm probing beam in the CS_2 Kerr medium. The 532 nm beam diameter is 1 mm and is located at the center of the 1064 nm pumping beam of 3 mm in diameter. The 1064 nm laser beam is directed into energy/power meter (D).

For a 6-cm length grating, the probing time base covered ~200 ps. Another lens collected the transmitted beam and focused it onto a CCD camera for analysis. The channel/pixel number of the CCD camera displayed the time is 1024. In this manner, ~1000 times divided data signals can be displayed for a single probing pulse to accurately monitor the temporal profile of the 1064 nm pulse offering a continuous display of the profile. The salient function of the blazed grating was also to compensate the probing pulse chirp due to the nonlinearity of the amplifier [8]. The probing pulse spectral width measured by a Jarrell-Ash scanning spectrometer was ~6.5 Å. The calculated minimum duration of the oblique front at given time was about 5 ps. The time covered by a CCD channel was 0.2 ps. Including the response time of the CS_2 Kerr medium, ~2 ps, this SOKG approach can measure the shape of a laser pulse (FWHM ~40 ps) with about 8 ps temporal resolution over a 200 ps time window.

Using a conventional OKG to measure the temporal profile of one pulse requires the movement a delay device to change the delay path between the gating and the probing pulses, and requires a large number of independent movements to form a profile [9]. Neglecting the response time of the Kerr medium, the minimum temporal resolution is determined by the time convolution of the gating pulse and the probing pulse for a conventional OKG. For the gating pulse of 40 ps and the probing pulse 30 ps, the minimum time resolution is ~1.4 times the FWHM of the gating pulse (the time convolution of the signal pulse and the gate pulse with ~ the same pulse width) which is 42 ps.

The pulse profile measurements for propagation through a ZnSe plate were performed to determine the pulse reshaping arising from nonlinear intensity-dependent processes. A set of neutral density filters (F) was used to control the power density for the 1064 nm pulse passing through the ZnSe plate. Neutral density filters were systematically switched between the entrance site and the exit site of the ZnSe sample. In this way, the 1064 nm intensity at ZnSe was varied, the total linear loss and the time delay of the experimental conditions were maintained to be about the same.

The measured SOKG temporal profiles of the transmitted 1064 nm pulse for incident pulse of

three different peak-power-densities: 0.365, 1.46 and 3.65 GW/cm^2 are displayed in Fig. 2. Intensity-dependent pulse shaping was observed. The salient features shown in Fig. 2 are pulse advancement and temporal pulse width shortening at high intensity. From 0.365 to 1.46 GW/cm^2, there was no profile distortion. From 1.46 to 3.65 GW/cm^2, the trailing portion of the original profile almost completely disappeared. In addition, (at 3.65 GW/cm^2) the profile peak moved forward ~15 ps and the FWHM was reduced to ~27 ps.

A 3 mm glass plate was used as a reference transparent optical material with a small $\chi^{(3)}$ nonlinearity. The measured temporal profiles for incident pulse with similar peak-power-densities are shown in the upper left inset of Fig. 2. These profiles seem to coincide without any pulse peak-shift and pulse compression. It shows good alignment of the experimental setup and good stability of the laser system. Using a 1 mm CS_2 cell instead of the ZnSe sample, changes in the measured profile were observed without pulse shaping. These changes originated from the self-focusing caused by the nonlinearity in CS_2. The observations in ZnSe imply that the pulse shaping does not only depend on the Kerr nonlinearity.

Typically, the nonlinear absorption of the 1064 nm laser by a pure ZnSe sample occurs by three-photon absorption because of its large band-gap energy of ~2.68 eV ($\lambda = 460$ nm). However, for the ZnSe sample used in this experiment, a commercial amorphous window, the transmission spectrum of this 3 mm thick ZnSe sample measured by a Perkin–Elmer Lambda 9 spectrometer is shown in the upper right inset of Fig. 2. Due to the large interface reflections of ZnSe, the measured transmissivities at 532 and 1064 nm are 52.85% and 67.31%, respectively. Taking into account the influence of surface reflection of ZnSe,

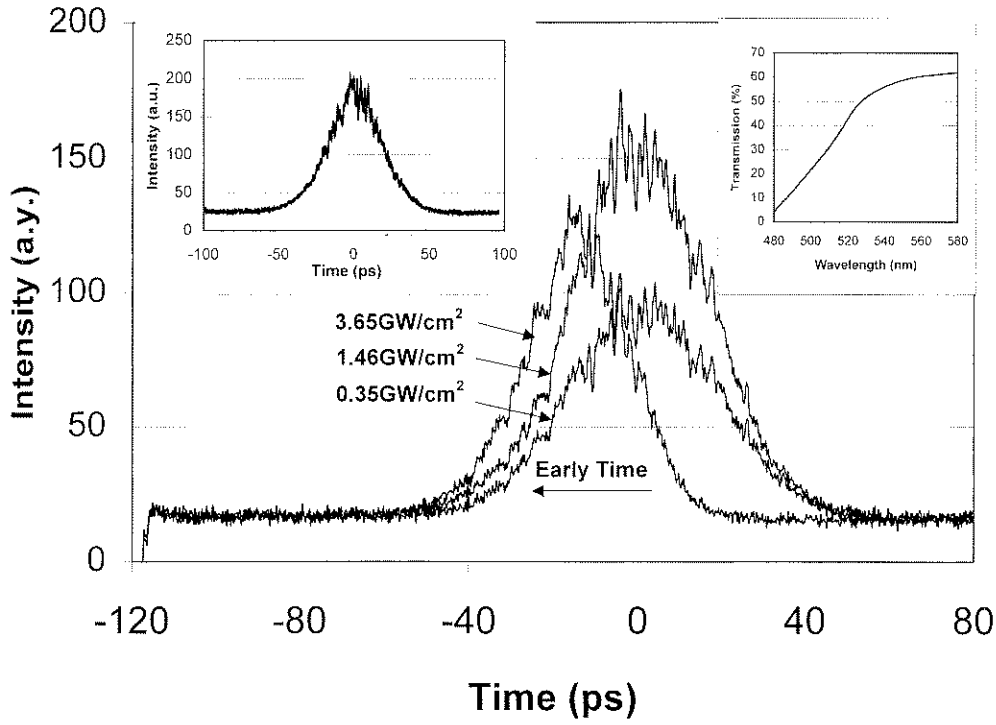

Fig. 2. Single-shot OKG temporal profiles of a 40-ps 1064-nm pulse passing through a 3 mm ZnSe plate when the peak intensity of the incident pulse reaches 0.365, 1.4, and 3.65 GW/cm^2. *Upper left inset*. Single-shot OKG temporal profiles of a 40-ps 1064-nm pulse passing through 3 mm glass at intensities 0.365, 1.46, and 3.65 GW/cm^2. *Upper right inset*. The transmissivity of a 3 mm ZnSe plate without coating as a function of wavelength.

the transmission at 532 nm is ~10%, while the absorption at 1064 nm is almost 0%. Since a strong absorption exists at 532 nm near the turning point of the transmission curve, two-photon absorption of 1064 nm in this ZnSe window sample is expected from tailing states.

For an incident pulse with the peak-power-intensity of 3.65 GW/cm^2, the instantaneous transmitted intensity of a single pulse with this incident intensity is shown in Fig. 3. This curve shows the difference in the output profile with intensity at different times with the pulse window. The transmission is the two-valued function of intensity. It indicates an operative complex nonlinear process. The transmission of the early leading part of the incident pulse is linear at the intensity level lower than 1.5 GW/cm^2. As the time of the intensity increases to the peak value, the transmitted intensity decreases and the trailing part of the pulse almost disappeared. Therefore, the nonlinear absorption of the 1064 nm laser pulse through ZnSe is not simple two-/three-photon absorption because the nonlinear absorption not only depends on intensity but also depends on time. The observed pulse shortening cannot be interpreted by a simple two-/three-photon absorption because two-/three-photon absorption at the center of pulse is large than at the wings causing a time broadening.

The intensity-dependent peak-shift of the laser pulse through ZnSe is attributed to intensity-dependent group-velocity. Using the expression for the intensity-dependent group-velocity [10], the measured peak-shift of $\Delta\tau = -15$ ps, and the known Kerr nonlinearity [4], $n_2(1064\text{ nm}) = 170 \times 10^{-9}$ esu, the nonlinear dispersion can be calculated to be $\partial n_2/\partial\omega \approx -1.53 \times 10^{-29}$ m^2 s/W.

To explain the two salient features observed at high pulse energy: pulse advancement and pulse shortening, we present a model based on two-step absorption with negative nonlinear dispersion. The energy level diagram of two-step absorption is illustrated in the inset of Fig. 4. Negative nonlinear dispersion results in the advancement and the leading edge steepening of the propagating pulse because the intensity-dependent group-velocity depends on nonlinearity and nonlinear dispersion [10]. The two-step process includes the single-photon absorption from a metastable state (one of gap states) which was populated by two-photon excitation. In this manner, two-step absorption results in the reduction of trailing portion of the propagating pulse because the linear absorption

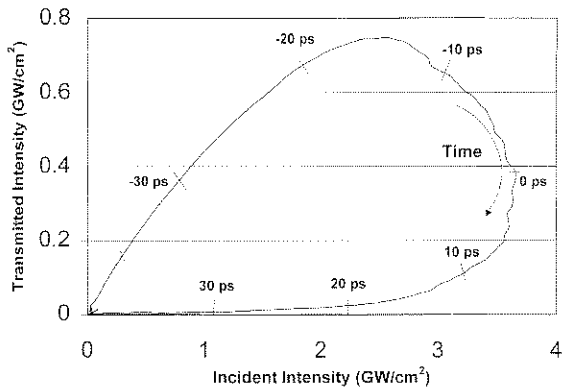

Fig. 3. The transmitted hysteresis of a single 1064 nm laser pulse through a 3 mm thick ZnSe plate at the peak intensity of an incident pulse of 3.65 GW/cm^2.

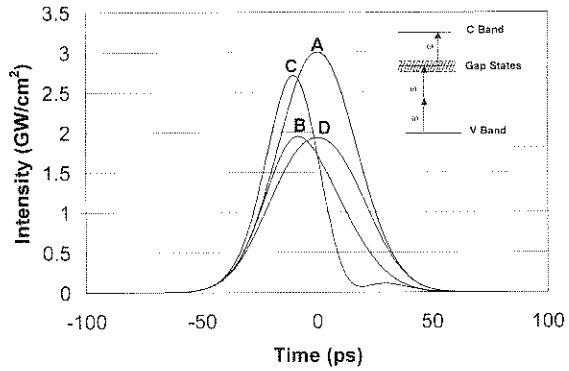

Fig. 4. Theoretical calculations: Curve A is the incident pulse with the Gaussian profile; curve B is the transmitted pulse after two-step absorption without nonlinear dispersion where $\sigma_{01}^{(2)}\sigma_{12}^{(1)}N = 4 \times 10^{-12}$ m/s/W^2 ($\sigma_{01}^{(2)}$ is the cross-section of two-photon absorption, $\sigma_{12}^{(1)}$ is the cross-section of gap states absorption and N is the occupation-number density); curve C is the transmitted pulse after two-step absorption with nonlinear dispersion where $\delta_{01}^{(2)}N = -3.8 \times 10^{-21}$ sm/W ($\delta_{01}^{(2)}$ is the additional nonlinear dispersion coefficient due to two-photon absorption); and curve D is the transmitted pulse after pure three-photon absorption where the coefficient of three-photon absorption, $\gamma = 4.6 \times 10^{-14}$ m^3/W^2. *Inset*. The energy level diagram of two-step absorption, two-photon absorption between valence band gap states and the delayed single-photon absorption from gap states to conduction band.

relies on the population in the metastable state excited by two-photon absorption from the leading edge photons [11]. The leading edge steepening and the reduction of the trailing portion of propagating pulse combine to produce the pulse shortening.

The effects arising from two-step absorption with negative nonlinear dispersion can be described by the following rate equations:

$$\frac{\partial}{\partial\tau}N_0 = -\frac{1}{2}\sigma_{01}^{(2)}(N_0 - N_1)I^2 + \frac{1}{T_{10}}N_1 + \frac{1}{T_{20}}N_2, \quad (1)$$

$$\frac{\partial}{\partial\tau}N_1 = \frac{1}{2}\sigma_{01}^{(2)}(N_0 - N_1)I^2 - \frac{1}{T_{10}}N_1 - \sigma_{12}^{(1)}(N_1 - N_2)I + \frac{1}{T_{21}}N_2, \quad (2)$$

$$\frac{\partial}{\partial\tau}N_2 = \sigma_{12}^{(1)}(N_1 - N_2)I - \frac{1}{T_{21}}N_2 - \frac{1}{T_{20}}N_2, \quad (3)$$

$$\frac{\partial}{\partial\xi}I = -\sigma_{01}^{(2)}(N_0 - N_1)I^2 - \sigma_{12}^{(1)}(N_1 - N_2)I - \delta_{01}^{(2)}(N_0 - N_1)I\frac{\partial}{\partial\tau}I - \delta_{12}^{(1)}(N_1 - N_2)\frac{\partial}{\partial\tau}I, \quad (4)$$

where the total occupation-number density is constant, $N = N_0 + N_1 + N_2$, and N_0, N_1 and N_2 are the occupational-number densities of the valence band, the gap states and the conduction band, respectively, I is the intensity of laser pulse, $\sigma_{01}^{(2)}$ is the cross-section of two-photon absorption, $\sigma_{12}^{(1)}$ is the cross-section of the gap states absorption, $\delta_{01}^{(2)}$ is the additional nonlinear dispersion coefficient due to two-photon absorption, $\delta_{12}^{(1)}$ is the additional linear dispersion coefficient due to gap states absorption, $\tau = t - z/v_g$ notes the retarded time, v_g is the group-velocity without absorption, $\xi = z$ notes a coordinate in the moving frame, T_{10} is the lifetime of gap states, T_{20} and T_{21} are the lifetimes of the conduction band relative to the valence band and gap states, t is the time, z is the distance. According to the conditions and approaches of Herrman et al. [11] reduces into

$$\frac{\partial}{\partial\tau}N_1 = \frac{1}{2}\sigma_{01}^{(2)}NI^2 - \frac{1}{T_{10}}N_1, \quad (5)$$

$$\frac{\partial}{\partial\xi}I = -\sigma_{12}^{(1)}(N_1 - N_2)I - \delta_{01}^{(2)}(N_0 - N_1)I\frac{\partial}{\partial\tau}I - \delta_{12}^{(1)}(N_1 - N_2)\frac{\partial}{\partial\tau}I. \quad (6)$$

For the ZnSe plate used in our experiment, the second term in the right-hand side of Eq. (5) and the third term in the right-hand side of Eq. (6) can be neglected because the lifetime of gap states is much longer than the width of incident pulse and the linear dispersion corresponding to the wide band absorption of gap states is small. Without nonlinear dispersion, the solution of Eqs. (5) and (6) is [11]

$$I(\xi,\tau) = \frac{I(0,\tau)}{1 + \frac{1}{2}\sigma_{01}^{(2)}\sigma_{12}^{(1)}N\xi\int_{-\infty}^{\tau}\mathrm{d}\tau' I^2(0,\tau')}. \quad (7)$$

In an increment $\Delta\xi$, the two-step absorption process with negative nonlinear dispersion can be approximately divided into two independent processes: absorption process and dispersion process. In the absorption process, the effect of negative nonlinear dispersion is neglected

$$I'(\xi + \Delta\xi,\tau) \approx \frac{I(\xi,\tau)}{1 + \frac{1}{2}\sigma_{01}^{(2)}\sigma_{12}^{(1)}N\Delta\xi\int_{-\infty}^{\tau}\mathrm{d}\tau' I^2(\xi,\tau')}. \quad (8)$$

In the dispersion process, the effect of two-step absorption is neglected

$$I(\xi + \Delta\xi,\tau) \approx I(\xi,\tau) - \frac{1}{2}\delta_{01}^{(2)}N\Delta\xi\frac{\partial}{\partial\tau}[I'(\xi + \Delta\xi,\tau)]^2. \quad (9)$$

Using the parameters: $\sigma_{01}^{(2)}\sigma_{12}^{(1)}N = 4\times10^{-12}$ m/s/W^2 and $\delta_{01}^{(2)}N = -3.8\times10^{-21}$ sm/W, and Eqs. (8) and (9), the transmitted pulse profiles were numerically simulated. The reshaping of the laser pulse profile upon passing through the ZnSe plate are shown in Fig. 4 for different conditions. Curve A is the incident pulse with the Gaussian profile; curve B is the transmitted pulse after two-step absorption without nonlinear dispersion; curve C is the transmitted pulse after two-step absorption with nonlinear dispersion. For contrast, curve D shows the transmitted pulse after pure three-photon absorption. It is clear that curve C posses the same salient features of the experimental profile at high intensity.

The time advancement and temporal narrowing of the picosecond pulse passing through ZnSe have been observed using our developed single-shot Kerr gate technique at the incident pulse

peak intensity of 3.65 GW/cm^2 in a ZnSe plate. The negative nonlinear dispersion was obtained based on the intensity-dependent peak-shift of the propagating pulse. Time-dependent transmission of a 1064 nm laser pulse through ZnSe shows that the nonlinear absorption in ZnSe at 1064 nm is not simply three-photon absorption process. Based on the model of two-step absorption with negative nonlinear dispersion, the main feature of the experimental results have been described.

Acknowledgements

This research is supported in part by AF Wright Laboratory, NYSTAR and ARO.

References

[1] G.R. Olbright, N. Peyghambarian, H.M. Gibbs, H.A. Macleod, F. Van Milligen, Appl. Phys. Lett. 45 (1984) 1031.

[2] I. Janossy, M.R. Taghizadeh, J.G.H. Mathew, S.D. Smith, IEEE J. Quantum Electron. QE-21 (1985) 1447.

[3] E.W. Van Stryland, H. Vanherzeele, M.A. Woodall, M.J. Soileau, A.L. Smirl, S. Guha, T.F. Boggess, Opt. Eng. 24 (1985) 613.

[4] M. Sheik-Bahae, D.C. Hutchings, D.J. Hagan, E.W. Van Stryland, IEEE J. Quantum Electron. QE27 (1991) 1296.

[5] M. Sheik-Bahae, A.A. Said, T. Wei, D.J. Hagan, E.W. Van Stryland, IEEE J. Quantum Electron. QE26 (1990) 760.

[6] K.W. Berryman, C.W. Rella, Phys. Rev. B 55 (1997) 7148.

[7] R.R. Alfano, Q.Z. Wang, T. Jimbo, P.P. Ho, R.N. Bhargava, B.J. Fitzpatrick, Phys. Rev. A 35 (1987) 459.

[8] E.B. Treacy, Phys. Lett. A 28 (1968) 34.

[9] P.P. Ho, R.R. Alfano, Phys. Rev. A 20 (1979) 2170.

[10] Yingxin Bai, Fanan Zeng, P.P. Ho, R.R. Alfano, Intensity-dependent group velocity, self-steepening and asymmetry of the spectral broadening of laser pulses in a nonlinear dispersion medium, to be submitted. (It gives the intensity-dependent group-velocity: $v_g(\omega, I) = c/(n + \omega\frac{\partial n}{\partial \omega} + 6n_2 I + \frac{3\omega}{n}(\frac{\partial (n_2 \omega)}{\partial \omega})I)$, and the time-delay of the pulse peak: $\Delta\tau = L/(c(6n_2 + \frac{3\omega}{n}(\frac{\partial (n_2 \omega)}{\partial \omega}))\Delta I)$, where $\Delta\tau < 0$ indicates the steepening of the leading-edge of the pulse, while $\Delta\tau > 0$ indicates the steepening of the trailing-edge of the pulse. In addition, $\Delta\tau/n_2 < 0$ gives a larger Stokes spectral broadening than anti-Stokes, and $\Delta\tau/n_2 > 0$ gives a larger anti-Stokes spectral broadening than Stokes.).

[11] J. Herrmann, J. Wieneeke, B. Wilhelmi, Opt. Quantum Electron. 7 (1975) 337 (In order to reduce the rate equations, two conditions are used: (1) the light intensity is only slightly changed by the two-photon absorption itself; and (2) the one-photon transition is supposed to affect the incident light strongly without being saturated.).